# Electronic Supplementary Information

# Insights into the role of nanoalloy surface composition toward catalytic acetone hydrogenation

Zhao Yang [a]*, Huaze Zhu [b], Huijuan Zhu [a], Yanbing Wang [a], liming Che [a]*, Zhiqing Yang [b]*, Jun Fang [c], Qi-Hui Wu [c], Bing Hui Chen [a]*

## Table of contents

**Experimental details**……2

Chemicals……2

Catalyst preparation……2

Catalyst characterization……3

Catalytic performance evaluation……4

**Summary of literature reported on catalytic acetone hydrogenation**……5

**Reaction pathways of acetone and 3-pentanone hydrogenations**……6

**The physicochemical properties of samples**……6

**XRD pattern of catalyst's support**……7

**$N_2$ adsorption-desorption isotherms**……8

**TEM images and the corresponding metal particle size distributions**……9

**Conversion values and experimental details for the TOF calculations**……10

**Effect of agitation speed on catalytic activity**……11

**Effect of catalyst amount on catalytic activity**……12

**Reactions at different time on stream**……13

**TEM images of the spent catalysts after hydrogenation reactions**……14

**Comparison of the spent catalyst's metal loading with fresh one's**……14

**XPS spectra with respective deconvolutions**……15

**Valence state distributions**……16

**Comparison of the activity before and after catalyst's reduction treatment**……16

**References**……16

## Experimental details

### Chemicals

$H_2$ (purity≥99.999%) and $N_2$ (purity≥99.999%) were purchased from Linde Gas Co. Ltd. (Xiamen, China). Carbon black (BLACK PEARLS 2000 LOT-1366221) was purchased from Cabot Corporation and used as the catalyst support. Acetone (purity≥99.5%) was purchased from Sinopharm Chemical Reagent Co. Ltd. 3-pentanone (purity≥98%) was purchased from Aladdin Industrial Corporation (Shanghai, China). All other reagents (NaOH, $RuCl_3$, $H_2PtCl_6$, Ethylene glycol and anhydrous ethanol and etc.) were supplied from Sinopharm Chemical Reagent Co. Ltd. (Shanghai, China).

### Catalyst preparation

Ethylene glycol (EG) reduction process (surfactant-free) was used to prepare a series of PtRu/C samples with fixed total theoretical metal loading (wt.% = 3%) but with different respective metal contents, namely 3Pt/C, 2.5Pt0.5Ru/C, 2Pt1Ru/C, 1.5Pt1.5Ru/C, 1Pt2Ru/C, 0.5Pt2.5Ru/C and 3Ru/C (labeled as xPtyRu/C here, where x and y denote the theoretical weight percentage loading of Pt and Ru, the percentage sign was removed for naming simplicity). For the synthesis of 1.5Pt1.5Ru/C, 0.6 g carbon black was dispersed in 45 ml ethylene glycol and treated with ultrasonic for 1h to form homogeneous slurry. Then 4.8 ml $RuCl_3$ ethylene glycol solution (1.90 mg/ml, concentration of Ru) and 5 ml $H_2PtCl_6$ ethylene glycol solution (1.85 mg/ml, concentration of Pt) were added and stirred for 1h. After adjusting the pH to 8 using NaOH ethylene glycol solution (52mg/ml), the final solution was kept at 180$^{o}$C in $N_2$ ambience under reflux-condensation for 3h. After cooling down to room temperature, the pH of solution was adjusted to 2.0 with hydrochloric acid solution and then was vigorously stirred for another 10 h. Finally, such slurry was filtered and washed repeatedly with deionized water until no chlorine ion was detected, then dried in a vacuum oven at 60 $^{o}$C for 10 h. After drying process, samples were heat treated at 300 $^{o}$C in $N_2$ ambience for 3 h. Similar to 1.5Pt1.5Ru/C synthesis described above, other samples with different metal loading ratios of Pt to Ru were prepared by adding different amount of such two metal precursor ethylene glycol solutions according to the theoretical metal loading calculated. Before catalytic evaluation, the catalyst needs to be carefully grinded as completely as possible using the agate mortar to minimize

the size of catalyst particle (the carbon black used here is relatively easy to grind). The actual metal loading was determined by inductively coupled plasma mass spectrometry (ICP-MS) using an Agilent ICP-MS 4500 instrument. Considering the possibility of surface oxidation of the catalysts when exposed to air for long time, catalysts were evaluated for catalytic performance within 15 min after their preparations. Samples need to be stored using the standard Schlenk techniques under dry nitrogen immediately after their preparations for further characterization use.

**Catalyst characterization**

Nitrogen adsorption-desorption measurement was performed on a Micrometrics ASAP2020 system at liquid nitrogen temperature. Brunauer-Emmett-Teller (BET) equation was used to calculate the specific surface areas. The average pore diameter and pore size distributions were determined by Barrett-Joyner-Halenda (BJH) method from the desorption branches of isotherms. The total pore volume depended on the absorbed $N_2$ volume at a relative pressure of approximately 0.99.

Powder X-ray diffraction (XRD) characterization was carried out using a Rigaku Ultima IV X-ray diffractometer with Cu Kα radiation (40 kV and 30 mA) of wavelength $\lambda = 0.15418$ nm. Step-scans were taken over a 2θ range of $30^o$-$90^o$ with a scanning rate of $2^o$/min.

Transmission electron microscope (TEM), high-angle annular dark-field scanning transmission electron microscopy (HAADF-STEM) and elemental line-scan/mapping analysis were performed on Philips Analytical FEI Tecnai 30 electron microscope with a field emission source operated at an electron acceleration energy of 300 kV. The average particle size was determined from TEM images by measuring more than 200 particles from several imaged areas.

X-ray photoelectron spectroscopy (XPS) was performed on the PHI Quantum 2000 Scanning ESCA Microprobe equipment using monochromatic $Al_{k\alpha}$ radiation (1846.6 ev) as the X-ray source. The measured spectra were fitted using a least-squares procedure to a product of Gaussian-Lorentzian functions. High-sensitivity Low-energy ion scattering spectroscopy (HS-LEISS) was collected on an Ion-TOF Qtac100 low energy ion scattering analyzer, $^{20}Ne^+$ ions with a kinetic energy of 5 keV and the current of 1.6 nA were applied.

**Catalytic performance evaluation**

The performances in catalytic acetone and 3-pentanone hydrogenations were evaluated with a stainless-steel high-pressure reactor (Parr 4848). Selected amount of catalyst and 10ml ketone (solvent free) were placed into the reactor, then sealed and purged with $N_2$ to remove the remnant air (the temperature inside the reactor is 28 $^oC$ during the $N_2$ purging and $H_2$ feeding process). Catalytic evaluation was conducted at selected temperature under 5.3 MPa $H_2$ pressure. The agitation speed was fixed at 500 rpm. When reaction was finished, the reactor was quickly cooled to room temperature in an ice-water bath (3-pentanone hydrogenation evaluation was performed at 50$^oC$, the rapid cooling step is necessary. Acetone hydrogenation was evaluated at room temperature, the rapid cooling step is not required). The catalyst sample was separated by centrifugation. The quantitative analysis of the products were performed on GC (Shimadzu GC 2010) equipped with DB-35 (60m x 0.32 mm) capillary column and a flame ionization detector (FID), GC-MS (Shimadzu GC-MS 2010) was used for qualitative analysis. The activity was calculated by means of the turnover frequency (TOF) expressed in moles of ketone transformed per moles of surface metal per second. Ketone conversion was controlled to be below 15% to obtain the TOF values.

PtRu particle's dispersion was calculated using the equation: $D_M=(6n_sM)/(\rho Nd_p)$, pondered from the metal loadings determined by ICP-MS and assuming an equal distribution of both metals in the particles. Where $n_s$ is the number of metal atoms at the surface per unit area (Pt:$1.12\times10^{19}/m^2$, Ru:$1.63\times10^{19}/m^2$). M is the atomic mass (Pt:195.08 g/mol, Ru:101.07 g/mol). ρ is the metal density (Pt:21.45 $g/cm^3$, Ru:12.1 $g/cm^3$), N is the Avogadro's number ($6.023\times10^{23}$at./mol), $d_p$ is the metal particle mean size measured by TEM. The average values of these parameters were used to calculate the metal dispersion of PtRu particles considering the molar ratio of Pt to Ru in the samples.

**Table S1** Summary of literature reported on catalytic acetone hydrogenation to isopropyl alcohol

| Ref. | Catalyst | Reaction Conditions | TOF ($s^{-1}$) | Selectivity [a] | Conversion |
|---|---|---|---|---|---|
| [1] | $Ir(0)_n$ nanoclusters + 5 Å molecular sieves | T=22°C, 2.7 atm $H_2$, reaction time = 6h | 0.32 | 100% | 100% |
| [1] | $Ir(0)_n$ nanoclusters + HCl | T=22°C, 2.7 atm $H_2$, reaction time =9h ( 95% conversion can be achieved in 2h) | 1.92 | 95% | 100% |
| [2] | Semihollow Pd NPs on indium tin oxide surface | T=28°C, reaction time= 6 min, ( $NaBH_4$ is used as the hydrogen source here ) | | 100% | 99.8% |
| [3] | Pd- NP-modified hybrid-film-patch | T=25°C,reaction time = 20min,solvent :hexane, ( $NaBH_4$ is used as the hydrogen source here ) | | 100% | 99.5% |
| [4] | Raney Ni | T=80°C | | 100% | 99.92% |
| [4] | Raney cobalt | T=120°C | | 99% | 82.5% |
| [5] | $[Ir(CO)(PPh_3)_2]ClO_4$ | Solvent: $CDCl_3$, T=70°C, reaction time=5h, 3 atm $H_2$, | | | 75% |
| [6] | $[Rh_2(CO)_3(dppm)_2]^{2+}$ | Solvent: $CD_2Cl_2$,T=70°C,3 atm $H_2$ | $1.1\times10^{-5}$ | | |
| [7] | 50%$Ni/Al_2O_3$ | T=100°C, 1 atm $H_2$ in vertical tube | | 100 | 90% |
| [8] | (8.6%-15.4%)$Ni/SiO_2$ | T=200°C,1atm $H_2$ in vertical tube | 11 | 99% | 35% |
| [9,10] | $CuCr_2O_4$ | T=75°C, 10 vol% acetone in hydrogen. | | | 35% |
| [11] | 1%$Pt/SiO_2$ | T=100°C | | 99% | 18% |
| [12] | 0.2%Rh0.2%Te/$Al_2O_3$ | T=100°C, 1atm $H_2$ | | 97% | 65% |
| [13] | 1%Pt/active carbon | T=100°C,.Atmospheric $H_2$, | 8.5 | 100% | 16.3% |
| [14] | 2.89%Ru/C | T=40°C, reaction time=40min, 5.5 MPa $H_2$ | 7.20 | 100% | 100% |
| **This work** | **1.5%Pt1.5%Ru/C** | **T=28°C, reaction time=6min, 5.3MPa $H_2$** | **46.39** | **100%** | **100%** |

[a] selectivity to isopropyl alcohol.

A range of heterogeneous or homogeneous catalysts have been reported in acetone hydrogenation to isopropyl alcohol at reaction temperatures ranging from room temperature to 200°C. When operated at room temperature (zero/low energy consumption), for the Ir(0)n nano-cluster catalyst (Table S1), 95% conversion can be achieved in 2h with the TOF of 1.92 $s^{-1}$. However, addition of HCl in this system can lead to the by-product generation. Semihollow Pd nanoparticles (NPs) on indium tin oxide surface showed the remarkable high catalytic efficiency by producing 99.8% of isopropyl alcohol within 6 min at 28°C (Table S1). However, $NaBH_4$ was used as the hydrogen source, besides the higher cost than hydrogen in commercial applications, addition of $NaBH_4$ would burden the purification and separation processes due to the

existence of Na and B in the products. For the Pd-NP-modified–hybrid-film-patch (Table S1), 99.5% conversion with 100% selectivity to isopropyl alcohol could be achieved in 20 min at 25°C, besides $NaBH_4$ added as the hydrogen source, hexane was chosen as the solvent which is not in line with the demand for green production. In this study, 100% conversion with 100% selectivity to isopropyl alcohol can be achieved at room temperature within a short reaction time, in which the hydrogen gas is used as the hydrogen source and the whole process is solvent free. Such process in this study is efficient and green relative to most of the systems reported.

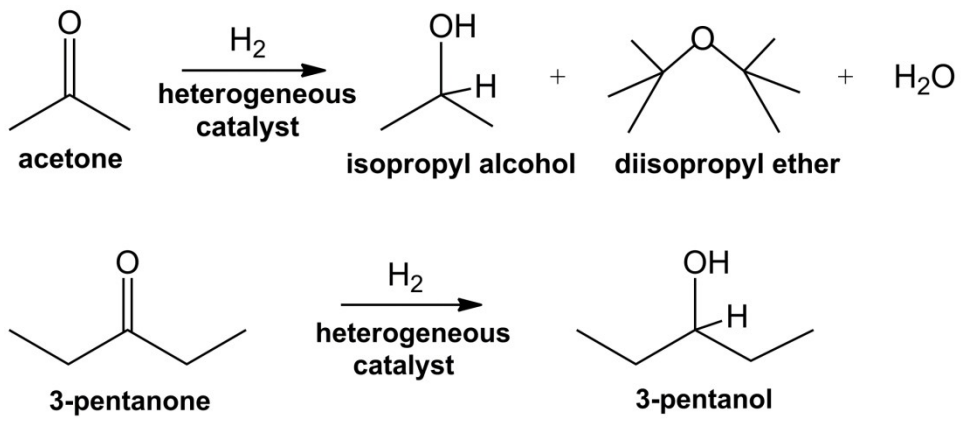


**Scheme S1** Reaction pathways of acetone and 3-pentanone hydrogenations established in this study.

**Table S2** Physicochemical properties of carbon supported PtRu nanoalloy catalysts with various compositions.

| Sample | Metal loading (wt.)[a] | Average particle size(nm) | | $S_{BET}$ ($m^2/g$) | $V_{pore}$($cm^3/g$)[d] | $D_{pore}$(nm) | Dispersion(%)[e] |
|---|---|---|---|---|---|---|---|
| | | By XRD[b] | By TEM[c] | | | | |
| 3Pt/C | 3.07%Pt | 6.2 | 6.45 | 1215.57 | 2.62 | 16.08 | 15.73 |
| 2.5Pt0.5Ru/C | 2.51%Pt 0.43%Ru | 4.2 | 4.04 | 1233.36 | 2.50 | 15.47 | 27.68 |
| 2Pt1Ru/C | 1.9%Pt 0.95%Ru | 3.0 | 2.87 | 1190.78 | 2.52 | 15.52 | 42.00 |
| 1.5Pt1.5Ru/C | 1.46%Pt 1.38%Ru | 2.7 | 2.71 | 1228.29 | 2.59 | 15.76 | 46.47 |
| 1Pt2Ru/C | 1.03%Pt 1.88%Ru | - | 2.17 | 1239.65 | 2.65 | 15.91 | 59.98 |
| 0.5Pt2.5Ru/C | 0.48%Pt 2.39%Ru | - | 2.33 | 1255.53 | 2.66 | 15.59 | 57.18 |
| 3Ru/C | 2.81%Ru | - | 2.62 | 1240.40 | 2.60 | 15.69 | 51.77 |
| C | - | - | - | 1385.95 | 3.03 | 16.17 | - |

[a] Detected by ICP-MS. [b] Determined by Scherrer equation. [c] See the statistical results of metal particle size in Fig.S3. [d] Obtained from $P/P_0$ = 0.99. [e] Calculated with the mean metal particle diameter from TEM statistical results in Fig.S3.

The actual metal loading is close to the preset value in the preparation. The grain size was calculated according to the FWHM of the strongest diffraction peak in

XRD pattern via Scherrer equation. The XRD pattern of the catalyst's support is shown in Fig.S1, due to overlapping with the broad characteristic peak of C (101) of catalyst's support, the strongest metallic diffraction peak Ru (101) of Ru could not quantitatively show the average grain size. Among these catalyst samples, their total pore volume and average pore diameter values vary insignificantly, indicating their similar pore structures and which is consistent with the similarity in their structures of $N_2$ adsorption-desorption isotherms shown in Fig.S2. BET results indicate that PtRu NPs are successfully deposited on the carbon black support without causing the obvious collapse of pore.

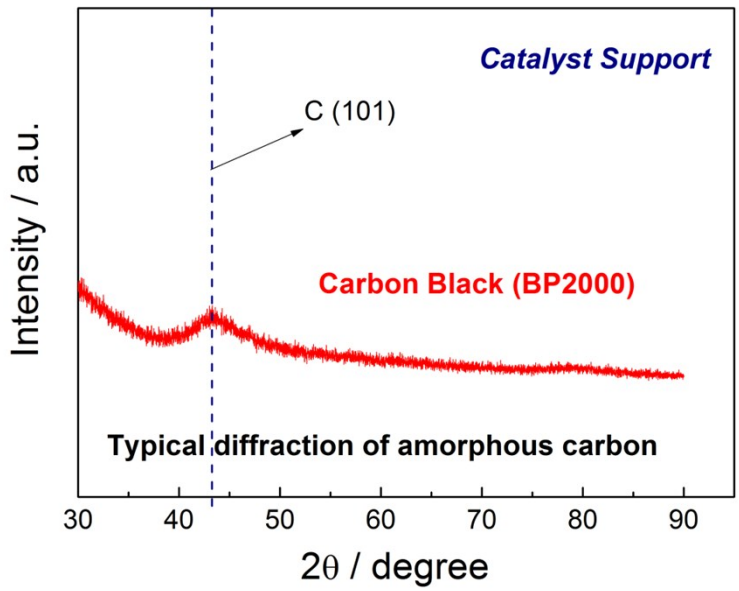


**Fig.S1** XRD pattern of catalyst's support (Carbon Black, BP2000)

Fig.S1 shows the appearance of broad diffraction peak of C (101) in the XRD pattern of catalyst's support (2θ value of C (101) = 43.5°), which is overlapped with Ru(101) diffraction peak (2θ value of Ru (101) = 44.0°, ICDD-JCPDS Card No. 06-0663) in 3Ru/C sample's XRD pattern shown in Fig.1a.

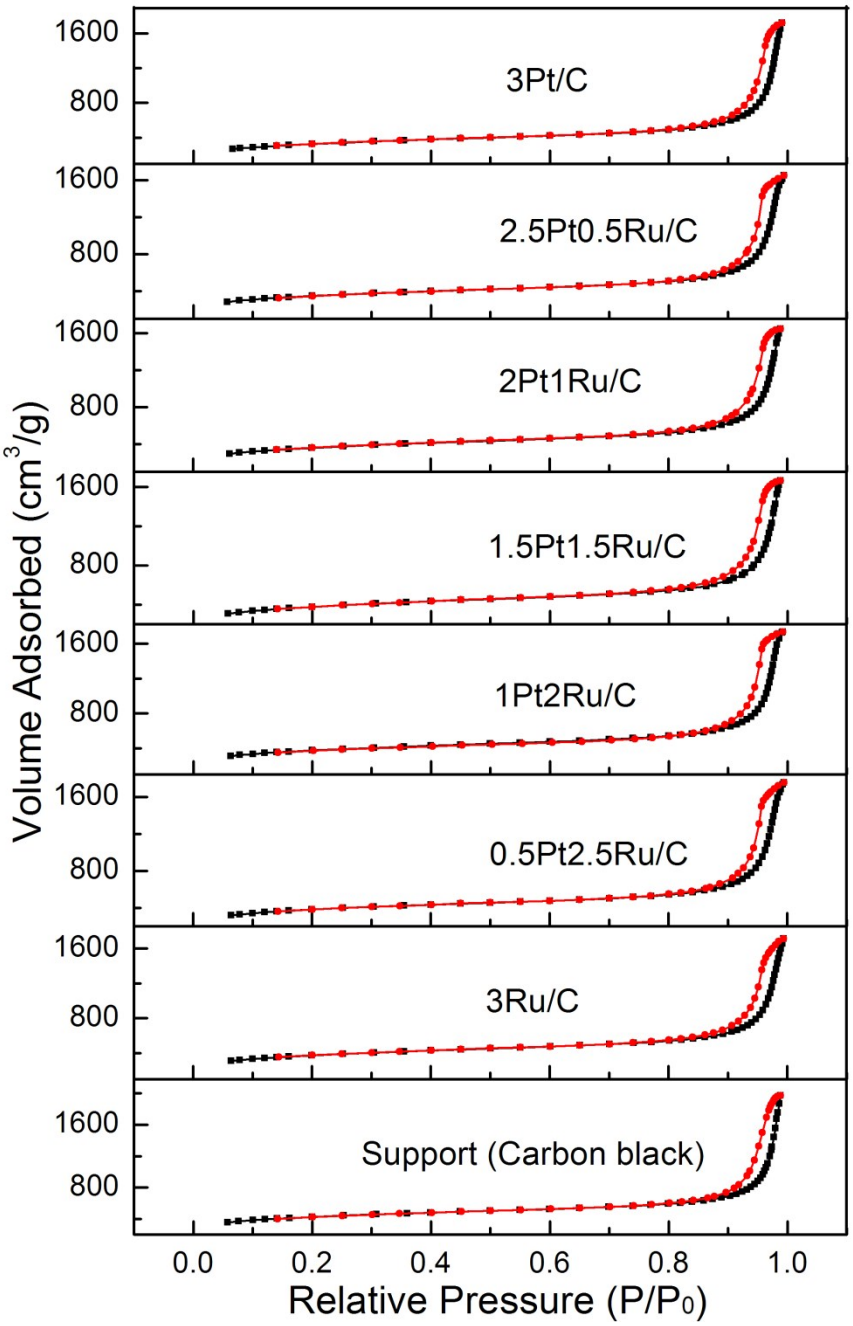


**Fig.S2** $N_2$ adsorption-desorption isotherms of carbon supported PtRu nanoalloy catalysts with various compositions.

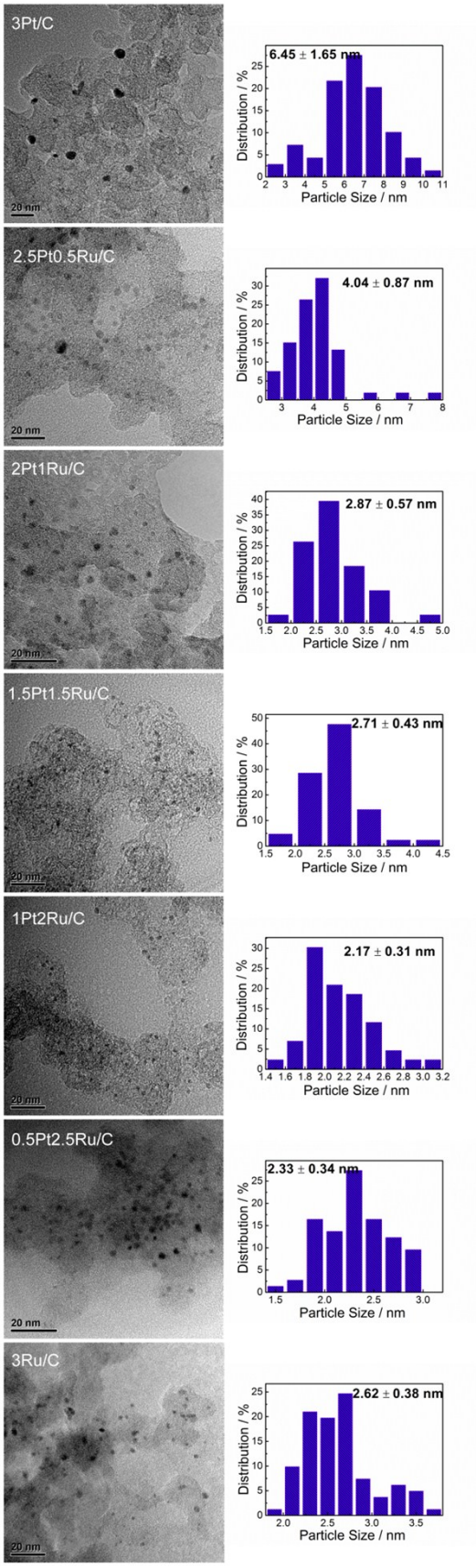


**Fig.S3** TEM images and the corresponding particle size distributions of carbon supported PtRu nanoalloy catalysts with various compositions.

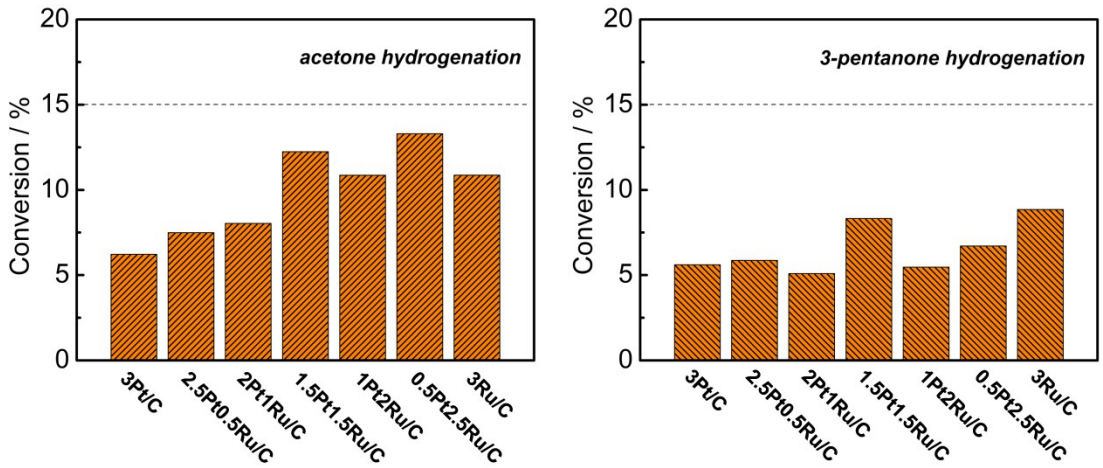


**Fig.S4** Catalytic conversion values of ketone hydrogenation on carbon supported PtRu nanoalloy catalysts with various compositions. The conversion values were controlled to be below 15%, related reaction conditions are shown as follows:

Reaction conditions for catalytic acetone hydrogenation on 3Pt/C: catalyst amount=100 mg, reaction time=6 min, $H_2$ pressure=5.3 MPa, reaction temperature= 28$^{o}$C, agitation speed=500 rpm. For 3-pentanone hydrogenation: catalyst amount=100 mg, reaction time=20 min, $H_2$ pressure=5.3 MPa, reaction temperature=50 $^{o}$C, agitation speed=500 rpm.

Reaction conditions for catalytic acetone hydrogenation on 2.5Pt0.5Ru/C: catalyst amount=25mg, reaction time=6min, $H_2$ pressure=5.3 MPa, reaction temperature=28 $^{o}$C, agitation speed=500 rpm. For 3-pentanone hydrogenation: catalyst amount=25mg, reaction time=20min, $H_2$ pressure=5.3 MPa, reaction temperature=50$^{o}$C, agitation speed= 500 rpm.

Reaction conditions for catalytic acetone hydrogenation on 2Pt1Ru/C: catalyst amount=10mg, reaction time=6min, $H_2$ pressure=5.3 MPa, reaction temperature=28 $^{o}$C, agitation speed=500 rpm. For 3-pentanone hydrogenation: catalyst amount=10mg, reaction time=20min, $H_2$ pressure=5.3 MPa, reaction temperature=50$^{o}$C, agitation speed=500 rpm.

Reaction conditions for catalytic acetone hydrogenation on 1.5Pt1.5Ru/C: catalyst amount=10mg, reaction time=6min, $H_2$ pressure=5.3 MPa, reaction temperature=28 $^{o}$C, agitation speed= 500 rpm. For 3-pentanone hydrogenation: catalyst amount=10mg, reaction time=20min, $H_2$ pressure=5.3 MPa, reaction temperature=50$^{o}$C, agitation speed=500 rpm.

Reaction conditions for catalytic acetone hydrogenation on 1Pt2Ru/C: catalyst amount=10mg, reaction time=6 min, $H_2$ pressure=5.3 MPa, reaction temperature= 28 $^oC$, agitation speed=500 rpm. For 3-pentanone hydrogenation: catalyst amount=10 mg, reaction time=20 min, $H_2$ pressure=5.3 MPa, reaction temperature=50 $^oC$, agitation speed=500 rpm.

Reaction conditions for catalytic acetone hydrogenation on 0.5Pt2.5Ru/C: catalyst amount=20 mg, reaction time=6 min, $H_2$ pressure=5.3 MPa, reaction temperature=28 $^oC$, agitation speed=500 rpm. For 3-pentanone hydrogenation: catalyst amount=20 mg, reaction time=20 min, $H_2$ pressure=5.3 MPa, reaction temperature=50 $^oC$, agitation speed=500 rpm.

Reaction conditions for catalytic acetone hydrogenation on 3Ru/C: catalyst amount =50 mg, reaction time=6 min, $H_2$ pressure=5.3 MPa, reaction temperature=28 $^oC$, agitation speed=500 rpm. For 3-pentanone hydrogenation: catalyst amount=50 mg, reaction time=20 min, $H_2$ pressure=5.3 MPa, reaction temperature=50 $^oC$, agitation speed=500 rpm.

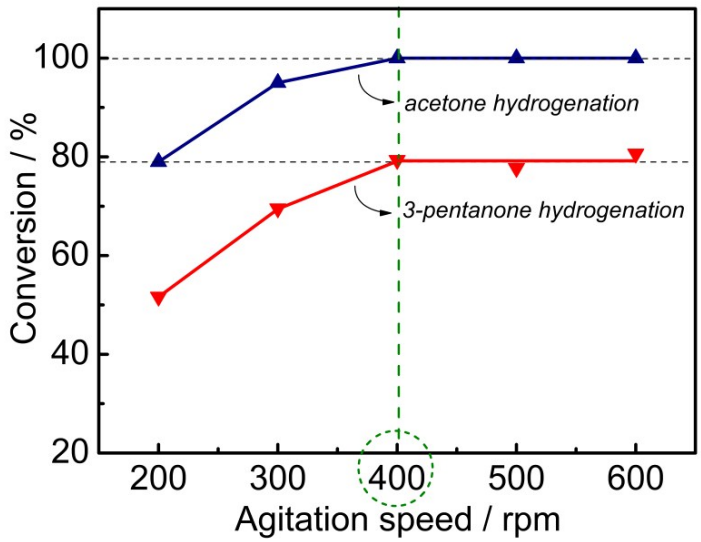


**Fig.S5** Effect of the agitation speed on catalytic activity (conversion) of ketone hydrogenation. 1.5Pt1.5Ru/C sample was used as the catalyst. Reaction conditions for acetone hydrogenation: catalyst amount=100 mg, reaction time=6 min, $H_2$ pressure=5.3 MPa, reaction temperature=28 $^oC$. For 3-pentanone hydrogenation: catalyst amount=100 mg, reaction time=20 min, $H_2$ pressure=5.3 MPa, reaction temperature=50 $^oC$.

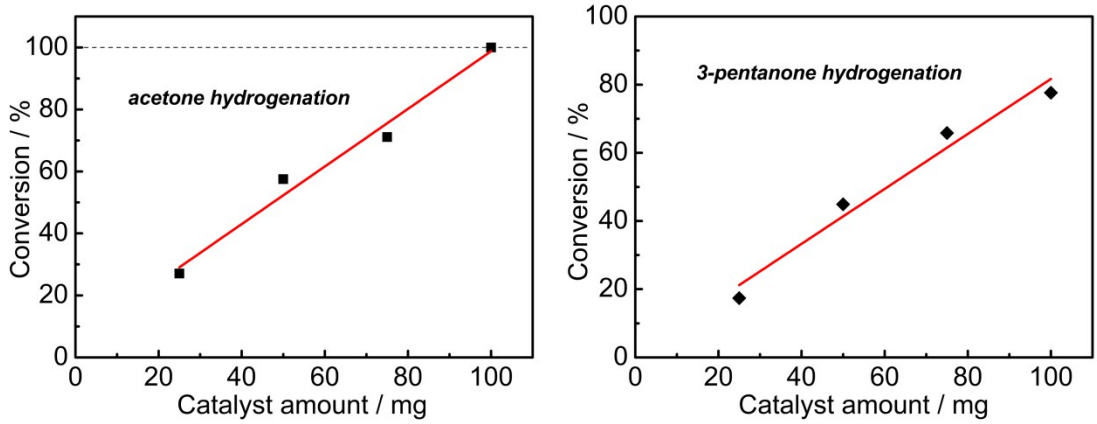


**Fig.S6** Effect of the catalyst amount added on catalytic activity (conversion) of ketone hydrogenation. 1.5Pt1.5Ru/C sample was used as the catalyst. Reaction conditions for acetone hydrogenation: agitation speed=500 rpm, reaction time=6 min, $H_2$ pressure=5.3 MPa, reaction temperature=28 $^{o}$C. For 3-pentanone hydrogenation: agitation speed=500 rpm, reaction time=20 min, $H_2$ pressure=5.3 MPa, reaction temperature= 50 $^{o}$C.

The heterogeneous catalysis can be significantly influenced by the mass transfer regime, including the internal and external diffusion processes. Studying the surface chemical reaction associated with the variation of catalyst structure needs to ensure that the catalytic evaluation conditions are not under mass transfer limitations. Generally, the intraparticle diffusion is largely influenced by the size of catalyst particle and the catalyst's pore diameter. The smaller size of catalyst particle and larger pore diameter can bring the lower influence of internal diffusion. In this study, carbon black (BP2000) was used as the catalyst's support, such carbon material possesses the relatively large pore diameter (16.17 nm, see Table S2), and is very easy to completely grind (which facilitates the minimization of the size of catalyst particle). The external diffusion process is largely influenced by the agitation speed, we performed the experiments to reveal the relationship between the agitation speed and the catalytic activity. As shown in Fig.S5, from 200 rpm to 400 rpm, the catalytic conversion of ketone increased with the agitation speed. From 400 rpm to 600 rpm, no obvious variation in catalytic activity was observed. Results indicate that when the agitation speed is lower than 400 rpm, the evaluation system appears to be limited by mass transfer (external diffusion). In order to avoid the mass transfer limitation, the catalytic evaluation experiments should be performed with the agitation speed > 400

rpm (500 rpm was selected in this study). Fig.S6 shows the effect of catalyst amount on catalytic activity, there is a clear linear association between the catalyst amount and the catalytic activity, such monodirectional increase of activity as catalyst amount increases indicates that the evaluation system is not under the mass transfer limitation (in the case of mass transfer limitation, the reactants transfer to catalyst surface is very slow in comparison with the surface catalyzed reaction, since mass transfer to catalyst surface is controlling, adding more catalyst could not significantly increase the reaction rates, due to the catalyst surface is not fully utilized in this case).

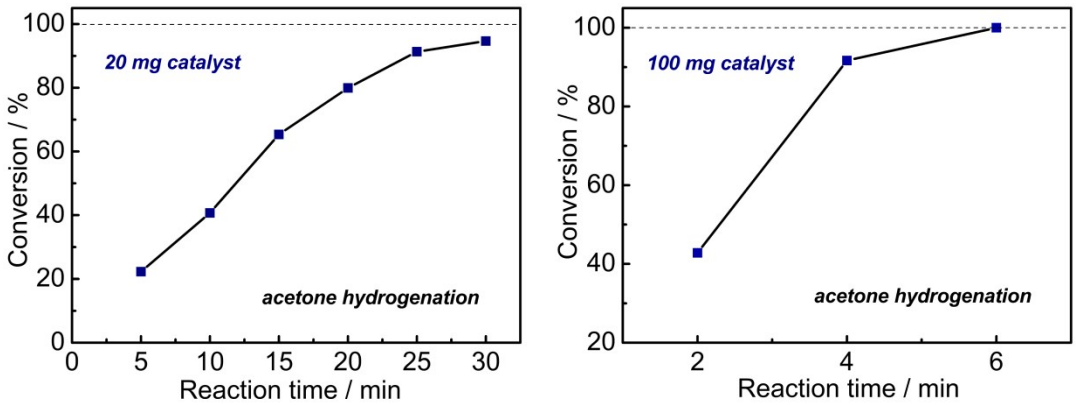


**Fig.S7** Catalytic acetone hydrogenation reactions at different time on stream. Two different amounts of 1.5Pt1.5Ru/C catalysts were selected. Reaction conditions: agitation speed=500 rpm, $H_2$ pressure=5.3 MPa, reaction temperature=28 $^{o}$C.

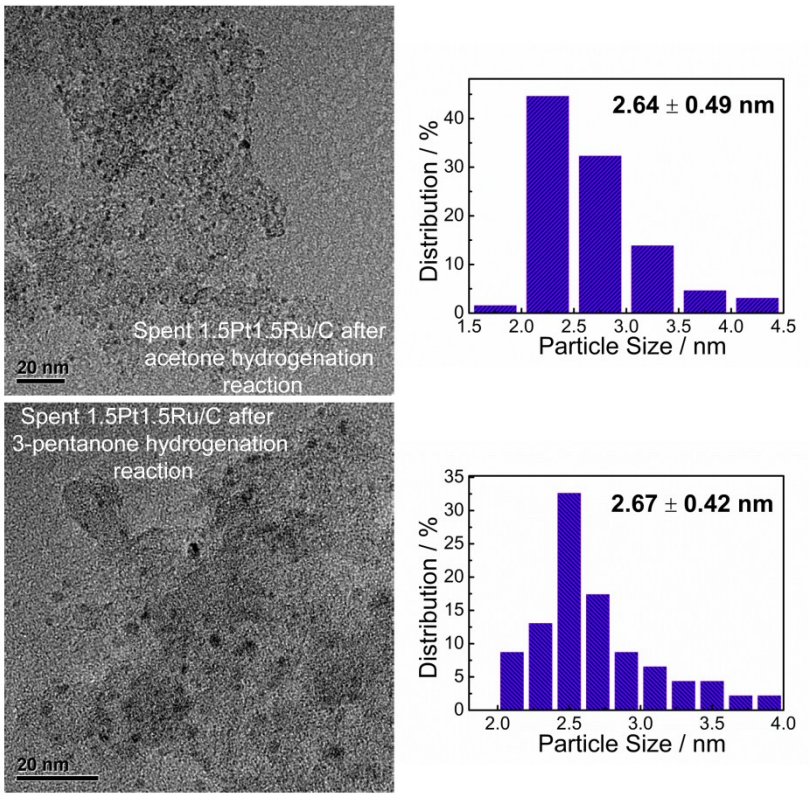


**Fig.S8** TEM images and the corresponding particle size distributions of spent catalysts after catalytic evaluations.

**Table S3** Comparison of the spent catalyst's metal loading with fresh sample's.

| Sample | Metal loading (wt.) [a] |
|---|---|
| fresh 1.5Pt1.5Ru/C | 1.46%Pt 1.38%Ru |
| spent 1.5Pt1.5Ru/C after acetone hydrogenation reaction | 1.41%Pt 1.32%Ru |
| spent 1.5Pt1.5Ru/C after 3-pentanone hydrogenation reaction | 1.39%Pt 1.34%Ru |

[a] Detected by ICP-MS. Reaction conditions are same as that in Table 1.

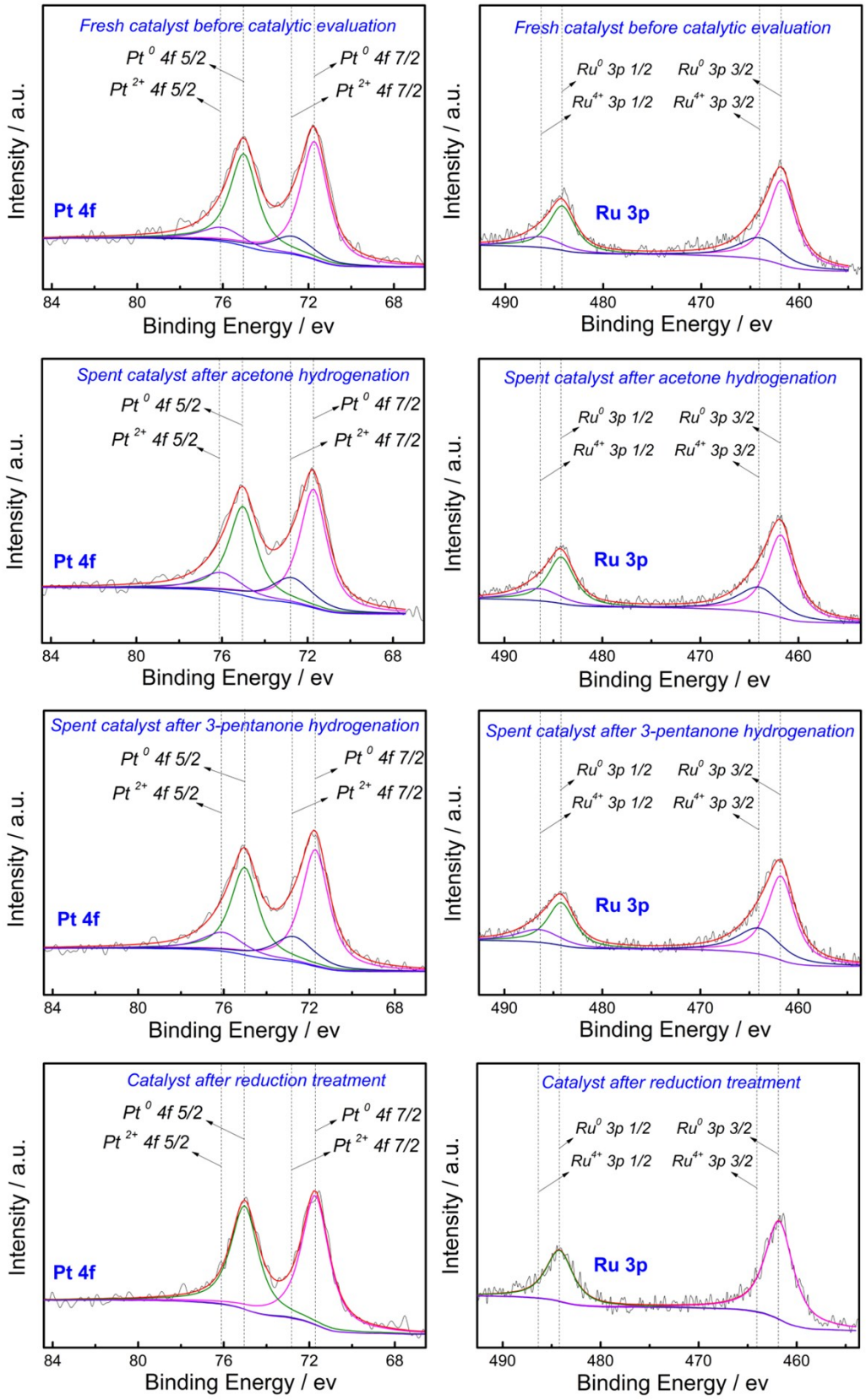


**Fig.S9** Pt 4f and Ru 3p XPS spectra with respective deconvolutions for 1.5Pt1.5Ru/C.

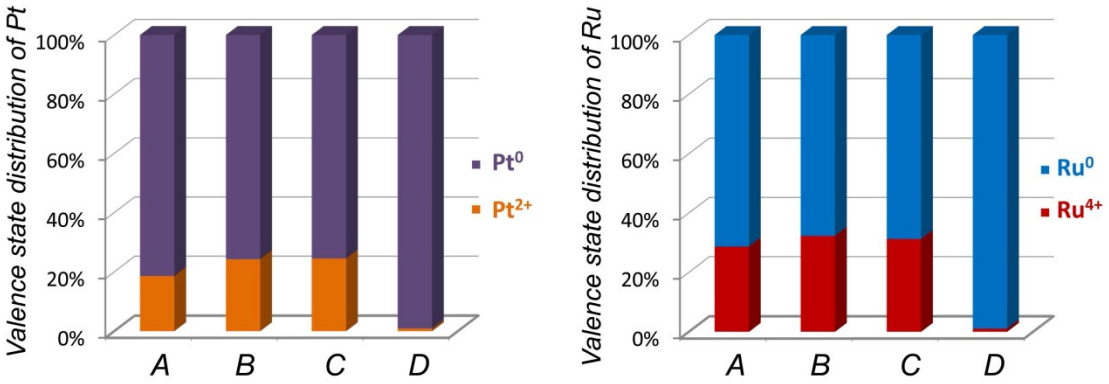


**Fig.S10** Valence state distributions from the deconvolutions of XPS spectrum for 1.5Pt1.5Ru/C. The corresponding Pt 4f and Ru 3p XPS spectra of these samples are shown in Fig.S4. Sample A: fresh catalyst before catalytic evaluation. Sample B: spent catalyst after acetone hydrogenation reaction. Sample C: spent catalyst after 3-pentanone hydrogenation reaction. Sample D: catalyst after reduction treatment, the fresh catalyst (after its heat treatment in $N_2$) was reduced in $H_2$ (atmospheric pressure) at 200°C for 1h.

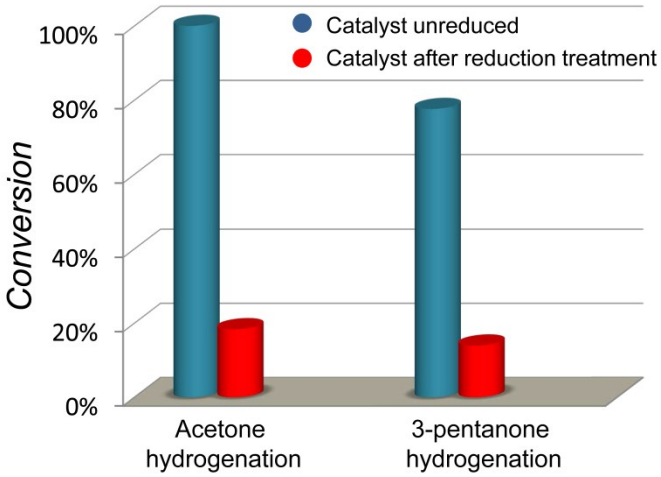


**Fig.S11** Comparison of the catalytic activity of 1.5Pt1.5Ru/C before and after its reduction treatment. The fresh catalyst (after its heat treatment in $N_2$) was reduced in $H_2$ (atmospheric pressure) at 200°C for 1h. Evaluation conditions are the same as that described in Table 1.

## References

1. S. Özkar and R. G. Finke, *Journal of the American Chemical Society*, 2005, **127**, 4800-4808.

2. A. Balouch, A. Ali Umar, A. A. Shah, M. Mat Salleh and M. Oyama, *ACS Applied Materials & Interfaces*, 2013, **5**, 9843-9849.

3. S. Ma, Y. Wang, K. Jiang and X. Han, *Nano Research*, 2015, **8**, 2603-2610.

4. K. S. P. M. Hayes, J. W. Mitchell, A. Niak, M. G. Turcotte, *U.S. Patent* **7041857B1**. May 9, 2006.

5. C. S. Chin, S. C. Park, *Bulletin of the Korean Chemical Society* 1988, **9**, 260-261.

6. F. Shafiq and R. Eisenberg, *Journal of Organometallic Chemistry*, 1994, **472**, 337-345.

7. S. Narayanan and R. Unnikrishnan, *Applied Catalysis A: General*, 1996, **145**, 231-236.

8. L. M. Gandia, A. Diaz and M. Montes, *Journal of Catalysis*, 1995, **157**, 461-471.

9. T. M. Yurieva, *Catalysis Today*, 1999, **51**, 457-467.

10. T. M. Yurieva, L. M. Plyasova, O. V. Makarova and T. A. Krieger, *Journal of Molecular Catalysis A: Chemical*, 1996, **113**, 455-468.

11. G. M. R. van Druten, L. Aksu and V. Ponec, *Applied Catalysis A: General*, 1997, **149**, 181-187.

12. N. N. Rimar and G. N. Pirogova, *Russian Chemical Bulletin*, 1998, **47**, 398-401.

13. A. M. Fuente, G. Pulgar, F. González, C. Pesquera and C. Blanco, *Applied Catalysis A: General*, 2001, **208**, 35-46.

14. Z. Yang, D. Li, L. Zhang, J. Zheng, N. Zhang and B. H. Chen, *ChemCatChem*, 2017, **9**, 338-346.